*Desalination and Water Treatment*
www.deswater.com

doi: 10.1080/19443994.2015.1108239

57 (2016) 20503–20510
September

Taylor & Francis
Taylor & Francis Group

# Photocatalytic decomposition of cyanide in pure water by biphasic titanium dioxide nanoparticles

Hossein Ijadpanah-Saravi[a], Saeed Dehestaniathar[b,*], Ahmad Khodadadi-Darban[a], Mehdi Zolfaghari[c], Saeed Saeedzadeh[d]

[a]*Faculty of Engineering, Environmental Engineering Department, Tarbiat Modares University, Tehran, Iran, Tel. +98 9303162646; email: hossein.ijad@gmail.com (H. Ijadpanah-Saravi), Tel. +98 9123908067; email: akdarban@modares.ac.ir (A. Khodadadi-Darban)*
[b]*Environmental Health Research Center, Kurdistan University of Medical Sciences, Sanandaj, Iran, Tel. +98 9127100637; email: saeed_dehestani@yahoo.com*
[c]*Department of Environmental Engineering, Institut national de la recherche scientifique, Quebec, Canada, Tel. +1 7607058888; email: mehdizolfaghari65@gmail.com*
[d]*Department of Polymer Engineering Color Technology, Amirkabir University of Technology, Tehran, Iran, Tel. +98 9366111977; email: ss.saeedzadeh@gmail.com*

Received 20 March 2015; Accepted 9 October 2015

ABSTRACT

Cyanide found in industrial wastes is among the critical environmental issues. The purpose of this research was to investigate the effects of various operating parameters, such as cyanide initial concentration, hydrogen peroxide dosage, amount of catalyst, UV light intensity and acidity on the photocatalytic degradation of cyanide using $TiO_2$ nanoparticles. The characterization of synthesized nanoparticles was also conducted using X-ray diffraction, and transmission electron microscopy techniques. Biphasic form of $TiO_2$ nanoparticles indicated the maximum removal yield and complete degradation of cyanide. Increase in initial concentration of cyanide causes decrease in removal yield. The complete removal of cyanide was achieved with dose of 3 mg $L^{-1}$ in 45 min, while lasting for 90 min without $H_2O_2$ degradation process. In addition, at pH 11 and catalyst content of 1 g $L^{-1}$, the maximum cyanide removal was observed. The efficiency of cyanide removal can be affected by various operating parameters. Increasing cyanide concentration resulted in decreasing removal rate of cyanide, as for concentrations 15 and 100 ppm cyanide was completely degraded during 10 and 90 min, respectively. Moreover, for cyanide degradation, the optimum $TiO_2$ content and pH were determined as 1 g $L^{-1}$ and 11, respectively. Furthermore, the efficiency of removal process corresponds with the increased UV lamp irradiation and $H_2O_2$ dosage.

*Keywords:* Cyanide; $TiO_2$ nanoparticles; Photocatalytic decomposition; Hydrogen peroxide dosage

*Corresponding author.

1944-3994/1944-3986 © 2015 Balaban Desalination Publications. All rights reserved.

## 1. Introduction

Nowadays, simple or complex forms of cyanide found in industrial wastes are among the critical environmental issues [1]. Cyanide is widely used for the recovery of valuable metals through cyanidation in the processing of mineral materials. Additionally, this material is abundant in the wastes of fiber production, coke factories, and petrochemical industry [2,3]. The allowable standard of this toxic substance is 2 ppm in waste, and concentration above 5 mg $kg^{-1}$ in human body results in death [4].

By now, various physical, chemical, and biological processes applied to remove cyanide content have faced some difficulties [3,5]. For physical methods, such as absorption and ion exchange, cyanide is merely saved in another form without being degraded. The general chemical methods applied using HClO and $Cl_2$ produce intermediate aromatic organic chlorides (AOX) which are highly toxic and needs further treatment process. Due to the toxic nature of these materials, biological method for removing cyanides is feasible only at low concentrations. In this regard, many researchers have recently focused on using novel methods such as advanced oxidation for cyanide removal [6–10]. In these researches, titanium dioxide ($TiO_2$) photocatalytic process was used as an advanced oxidation process (AOP) for cyanide degradation. $TiO_2$ molecules are excited by absorbing high-energy photons. Because of this excitation process, the electron from valence band is transferred to conduction band and an electron-hole pair is formed. Then, electron receptive species such as oxygen absorb the electron at catalyst surface and produces a superoxide radical. Besides, the remaining hole absorbs one electron from $OH^-$ ion in the medium and the hydroxide ion is generated. The created radicals oxidize the cyanide [11–14].

Auguliaro found that the radicals generated by $TiO_2$ are strong oxidizers for cyanide degradation [15]. Besides, Dąbrowski also showed that titanium dioxide ($TiO_2$) photocatalytic process has a high yield in the removal of simple and complex cyanides [1]. So far, a large number of studies have been conducted on photocatalytic removal of cyanide using $TiO_2$ nanoparticles [1,15–27]. However, while the methods proposed by these studies suffer from complexity and use of great deal of energy, they are not highly efficient as well. Consequently, these approaches are not practically feasible.

In another research, the authors of the present work used $TiO_2$ nanoparticles in the biphasic mix form of anatase and rutile (simultaneously synthesized from titanium tetrachloride) for cyanide removal. Using the biphasic mix of rutile with anatase could enhance the photocatalytic properties of anatase [28]. This increase can be attributed to the fact that anatase and rutile phases being together may accelerate the separation of positive and negative charges and postpones their recombination; and once rutile content is zero a slight drop in the photo activity rate is observed [28–30]. They also found that the biphasic anatase and rutile mix with $A/R = 4$ posed to 30 UV-C irradiation indicated the maximum catalytic properties in cyanide degradation as compared to the crystalline rutile and anatase phases (Fig. 1). Furthermore, calculating the process efficiency and consumed electric energy for various crystalline forms of $TiO_2$, it was revealed that the biphasic form of $TiO_2$ nanoparticles offers maximum output and minimum energy use.

Although cyanide removal by the presented method demonstrates high performance, there also exists different operational parameters affecting efficacy of this method for cyanide removal; for example, cyanide initial concentration, hydrogen peroxide dosage, amount of catalyst, UV light intensity, and acidity. The main objective of this work is to investigate the effect of these parameters on cyanide removal performance of the synthesized nanoparticles.

## 2. Materials and methods

### 2.1. Materials

The chemicals used in this work, all of which had high purification level (≥99%), are titanium tetrachloride, ammonium hydroxide, ammonium sulfate, hydrochloric acid, sodium cyanide, and sodium hydroxide were purchased form Merck Co., Germany. Table 1 presents the properties of synthesized nanoparticles.

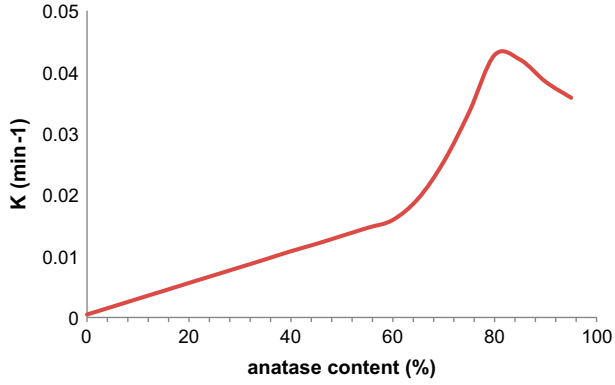



Fig. 1. The effect of anatase percent to photoactivity of titanium dioxide [28].

Table 1
Properties of the synthesized catalysts

| Properties | Type of nano-$TiO_2$ | | |
|---|---|---|---|
| | *A* | *A*/*R* = 4 | *A*/*R* = 1 |
| Anatase content (wt%) | 100% | 50% | 80% |
| Average crystallite size (nm) | 18.2 | 21.4 | 19.6 |
| BET surface area ($m^2\ g^{-1}$) | 94.86 | 60.79 | 85.32 |
| Total pore volume ($cm^3\ g^{-1}$) | 0.2397 | 0.1969 | 0.2147 |

### 2.2. Nanoparticles synthesis

Nanoparticles were synthesized using the controlled hydrolysis of $TiCl_4$ [28].

### 2.3. Characterization of nanoparticles

Several techniques were applied to characterize the properties of the used nanoparticles. In this regard, the crystalline phase and particle size was studied using X-ray diffraction (XRD) analysis by X'PERT 1480 device, Phillips, the Netherlands and average particle size was calculated using Debye–Scherrer equation [31]:

$$D = \lambda K/\beta \cos\theta \quad (1)$$

where $D$ is the mean particle diameter in nm; $K$ is a constant; $\lambda$ is X-ray wavelength; and $\beta$ is width of highest peak at half height in radian; and $\theta$ is the angle in which peak is observed.

To study $TiO_2$ nanoparticles, transmission electron microscopy (TEM), model: EM10C 80 KV, Zeiss, Germany, was utilized. The surface area was measured by Brunauer–Element–Teller (BET) method and nitrogen gas absorption at 77.15 K by COULTER SA3100 device.

### 2.4. Photoreactor

Degradation reactions of cyanide were performed through the UV/$TiO_2$ process inside a photo-reactor. The applied photoreactor system involves a cylindrical reactor containing an irradiation and an aeration system (Fig. 2). The reactor, with height and diameter of 35 and 20 cm, respectively, was equipped with a UV-C 30 watt lamp manufactured by Phillips Co.

## 3. Methodology and analysis

To initiate the required photocatalytic tests, at the beginning the solution containing cyanide and $TiO_2$ nanoparticles was required to reach equilibrium after 30 min at the dark. Once the equilibrium state was reached, for complete scattering of the particles the obtained solution was subjected to the ultrasonic waves for 15 min, then the UV light was turned on, and the final product was constantly agitated by a magnetic agitator. At the time intervals of 10 min, sampling process was performed for cyanide analysis. In addition, to remove $TiO_2$ nanoparticles, the samples were centrifuged with rotation rate of 4,000 RPM for 30 min. Besides, to avoid sunlight the samples were kept in a dark chamber. Cyanide concentration was measured using the titration method according to EPA9014 standard, the titration procedure introduced in the textbook "Standard Methods for Water and Wastewater Tests." To do so, first, 0.04 and $1.92 \times 10^{-2}$ solutions of sodium hydroxide and silver nitrate and a 20% rhodanine in acetone solution were prepared. Next, the final solution, which was 0.1 mL of the solution, was diluted by NaOH solution and its volume reached 10 mL, and next 0.5 mL of rhodanine was added to it. To carry out titration process, silver nitrate was added to the solution by drops until its color changed from yellowish to bright rose color. Cyanide content in the solution was measured using the following equation [32]:

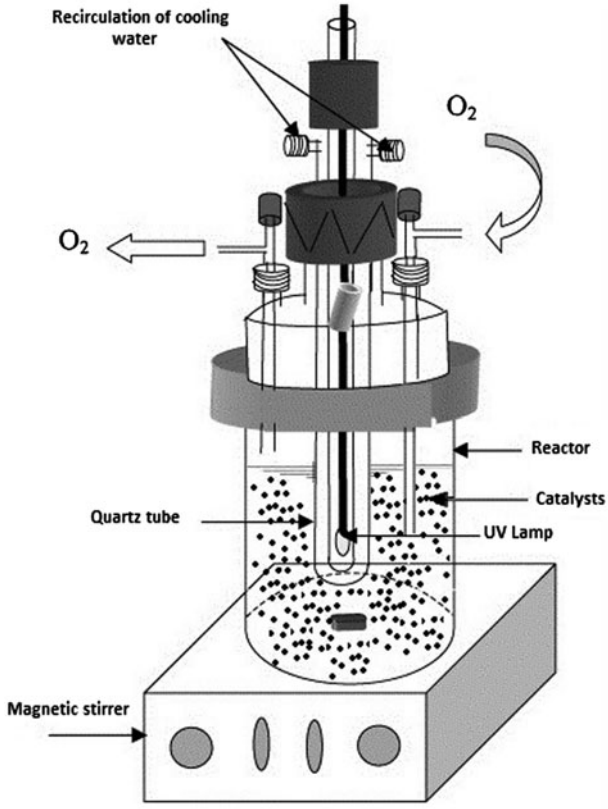



Fig. 2. Schematic drawing of the photoreactor.

$$C = 49.92(V - V_b) \quad (2)$$

where $C$ cyanide concentration in mg $L^{-1}$; $V$ volume of silver nitride used for color change in the final solution; and $V_b$ volume of sodium hydroxide.

## 4. Results and discussion

### 4.1. Catalyst characterization

#### 4.1.1. XRD test

Fig. 3 presents XRD pattern of $TiO_2$ nanoparticles in the crystalline anatase and rutile forms where $A/R = 4$. As shown in the figure, the sharpest peaks for the crystalline anatase form are observed at 25.5, 37, and 48.5 $cm^{-1}$. Also, the sharpest peaks for the crystalline rutile phase are at 27.5, 36, and 54.5 $cm^{-1}$. In this regard, Lee and Yang reported similar results [33]. Using the Debye–Scherrer equation, the mean diameter of the nanocrystalline anatase and rutile phases were calculated as 18.2 and 23.6 nm, respectively. Moreover, the surface area (BET) of anatase and rutile was obtained as 94.86 and 46.38 $m^2\ g^{-1}$, respectively.

#### 4.1.2. Transmission electron microscopy

In this research, TEM device was used to observe $TiO_2$ nanocrystals. As shown in Fig. 4, the synthesized nanoparticles have a mean diameter of 18–22 nm. Besides, the figure confirms that synthesized nanoparticles are completely separated and placed in the solution in a segregated fashion. The average particle size measured by TEM and XRD analysis were in good agreement.

### 4.2. Effect of initial cyanide content

Fig. 5 presents the effect of photodegradation for the various cyanide concentrations, in which the maximum yield occurred at 15 mg $L^{-1}$ where the complete degradation took place at duration shorter than 10 min. In addition, for the concentration of 500 mg $L^{-1}$, after 3 h, the final cyanide content reached to 150 mg $L^{-1}$. The results indicated that an increase in cyanide content leads to decrease in cyanide removal yield. This reduction can be attributed to the formation of multilayer cyanide around the catalyst at high concentrations. This multilayer imposes some

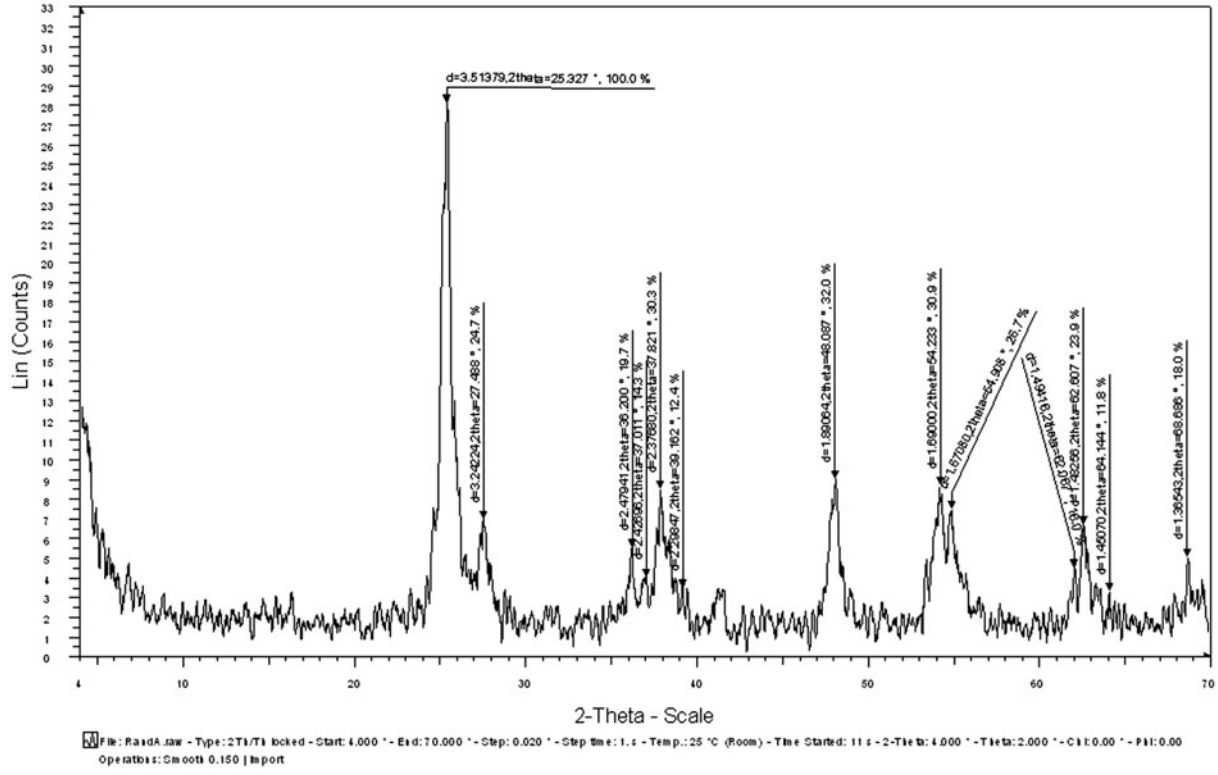



Fig. 3. XRD pattern of $TiO_2$ catalyst.

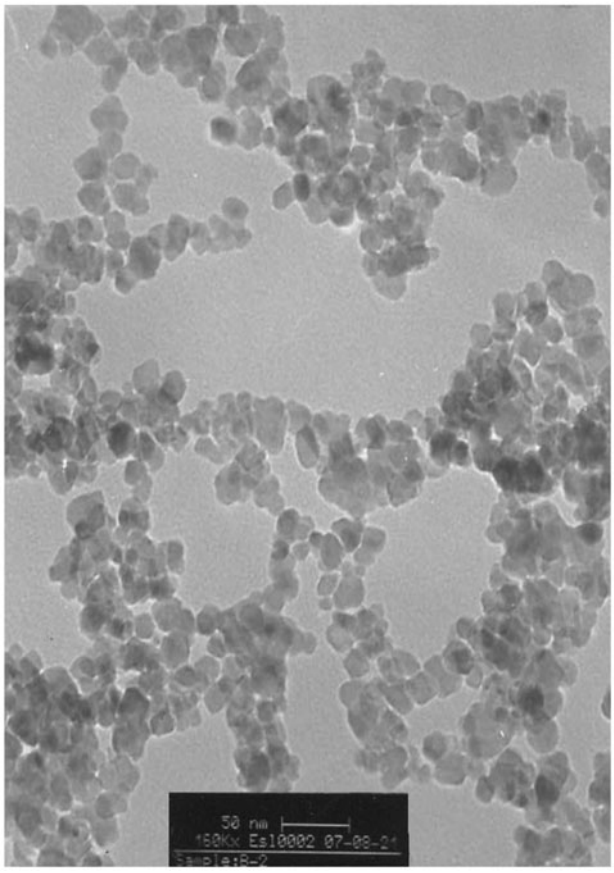



Fig. 4. TEM micrograph of nano-$TiO_2$ particle.

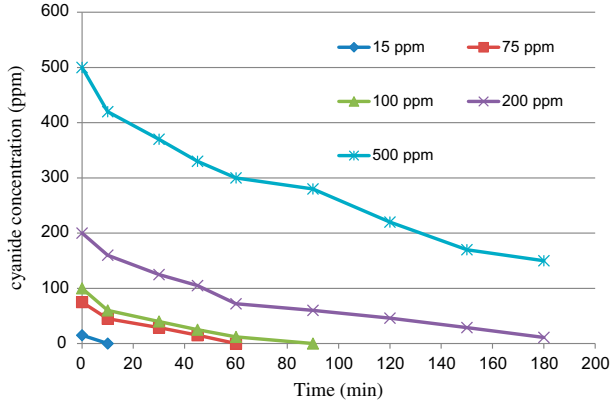



Fig. 5. The effect of the initial concentration of cyanide on its photocatalytic degradation.

interruptions in OH radical release. Moreover, high concentration of contaminant reduces photon penetration depth and, consequently, generation rate of OH radicals [2].

### 4.3. Effect of catalyst content

Fig. 6 illustrates the effect of catalyst content on cyanide removal, where increasing catalyst content up to 1 g $L^{-1}$ leads to an increased removal rate of cyanide. Also, once catalyst content rises from 1 to 2 g $L^{-1}$, cyanide removal rate gradually decreases; so, maximum cyanide removal percentage occurs at 1 g $L^{-1}$ cyanide concentration. Furthermore, the excessive decrease in catalyst content in the environment leads to two conditions; a: opacity and reduced penetration ability of the photon in the solution; and b: rising the probability of nanoparticles collision and particles integration and, as a result, decreased catalyst surface. Therefore, it can be stated that increase in the concentration of cyanide from 1 to 2 g $L^{-1}$ results in decrease of cyanide removal rate.

### 4.4. Effect of $H_2O_2$ dosage

Effect of $H_2O_2$ dosage on photodegradation of cyanide is shown in Fig. 7, where increasing $H_2O_2$ dosage leads to an increased cyanide removal percentage as cyanide is completely removed during 45 min at $H_2O_2$ dosage of 3 mg $L^{-1}$. The process takes 90 min in absence of $H_2O_2$. Here, the dosage of 3 mg $L^{-1}$ is selected as the optimum amount of $H_2O_2$. The following three phenomena are responsible for the accelerated oxidation of cyanide when adding $H_2O_2$ to the solution:

(a) The homogeneous dark oxidation of cyanides by $H_2O_2$.
(b) The impact of UV photons with $H_2O_2$ which enhances the number of generated OH radicals, and then, $H_2O_2$ photolysis process results

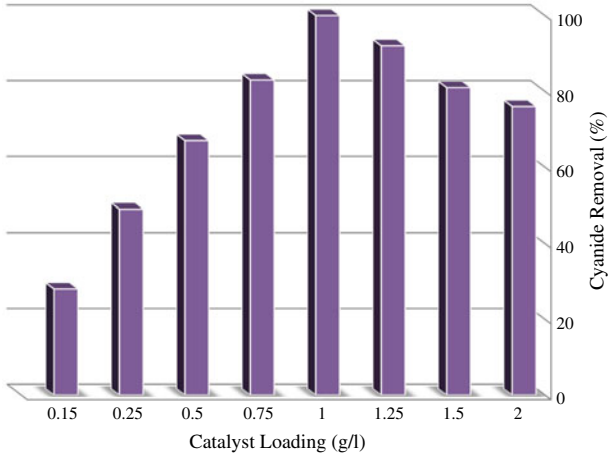



Fig. 6. The effect of catalyst content on photocatalytic degradation of cyanide.

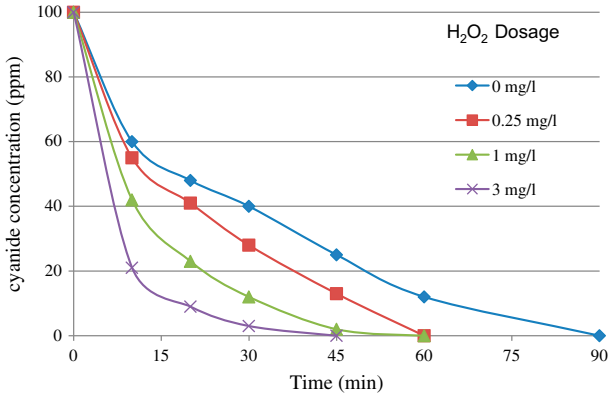



Fig. 7. The effect of $H_2O_2$ dosage on photocatalytic degradation of cyanide.

in further cyanide removal. The following equations represent the steps of OH radical generation by the addition of $H_2O_2$:

$$H_2O_2 \rightarrow 2OH^{\cdot} \quad (3)$$

$$H_2O_2 + e^- \rightarrow OH^- + OH^{\cdot} \quad (4)$$

(c) The photocatalytic degradation of cyanide by $TiO_2$ nanoparticles [3].

### 4.5. Effect of irradiation intensity of UV lamps

In this research, the effect of irradiation intensity of UV lamps on cyanide removal rate was studied under the conditions of 100 ppm cyanide concentration and catalyst dosage of 1 g $L^{-1}$ in the absence of $H_2O_2$. In general, the energy of UV photons is controlled by their wavelength; thus, the total energy of photocatalytic process depends on the intensity of the irradiate UV light. Once a greater deal of UV photons are irradiate on $TiO_2$ surface, a larger number of electrons are excited in valence band, leading to the release of more OH radical. Therefore, it is clear that the enhanced UV irradiation increases cyanide removal percentage. Fig. 8 presents the effect of UV irradiation intensity on cyanide removal yield.

### 4.6. Effect of initial pH

The solution pH has complicated effects on oxidation reaction of the materials. However, this parameter is generally controlled by the type of pollutant and electrostatic force in catalyst and pollutant interface. Fig. 9 demonstrates the pH and various amounts of $TiO_2$ nanoparticles effect on cyanide removal. As shown in the figure, the optimum pH for cyanide removal is 11. As the amount of generated OH radicals increases at alkaline $pH_s$ ($h^+ + OH^- \rightarrow$ OH), by rising pH up to 11, cyanide removal percentage increases. At pH 11, cyanide is entirely in ionic form, but at pH > 11, because of the competitive absorption between $CN^-$ and $HO^-$, the cyanide removal rate decreases; hence, the maximum cyanide removal occurs at pH 11.

### 4.7. Cyanide degradation trend

As previously mentioned, the impact of high-energy UV photons on valence layer electrons in $TiO_2$ excites their electrons and results in formation of positive holes and electrons with negative charge (reaction 1). Each of these centers can initiate a chain of reactions and produce related radicals by water and oxygen absorption (reactions 3 and 4) and produce heat by recombination (reaction 2):

$$TiO_2 \xrightarrow{h\vartheta} h^+ + e^- \quad (5)$$

$$h^+ + e^- \rightarrow \text{heat} \quad (6)$$

$$h^+ + H_2O \rightarrow OH^{\cdot} + OH^- \quad (7)$$

$$e^- + O_2 \rightarrow O_2^{\cdot} \quad (8)$$

Cyanide ion also can be independently absorbed by the hole and generate cyanide radical (reaction 5):

$$CN^- + h^+ \rightarrow CN^{\cdot} \quad (9)$$

By preceding the oxidation process and different reactions between cyanide radicals, first cyanogen and

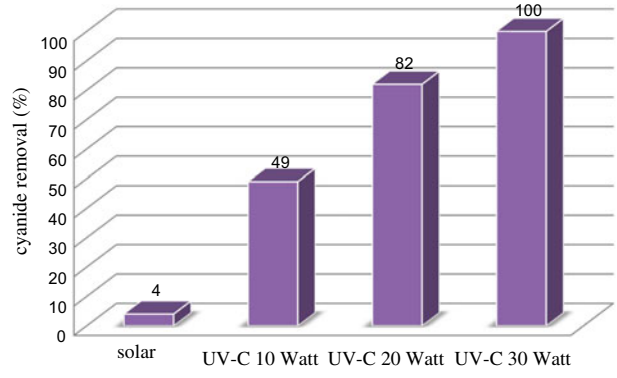



Fig. 8. The effect UV irradiation intensity on cyanide removal yield.

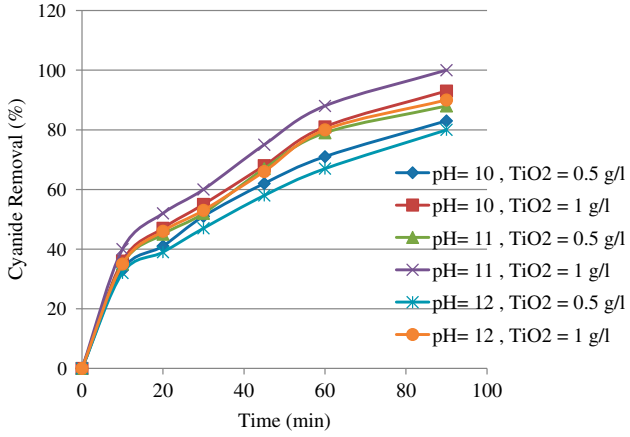



Fig. 9. The effect of acidity and $TiO_2$ nanoparticles content on photocatalytic degradation of cyanide.

then cyanate ion are generated (reactions 6 and 7). Also, the final product of hydroxide radical reaction with cyanide ion and intermediate components is cyanate ion:

$$CN^{\cdot} + CN^{\cdot} \rightarrow (CN)_2 \quad (10)$$

$$(CN)_2 + 2OH^{\cdot} \rightarrow CNO^{-} + CN^{-} + H_2O \quad (11)$$

$$CN^{-} + 2OH^{\cdot} \rightarrow CNO^{-} + H_2O \quad (12)$$

$$CN^{-} + OH^{\cdot} \rightarrow OHCN^{-\cdot} \rightarrow CONH^{-\cdot} \quad (13)$$

$$2CONH^{\cdot -} \rightarrow CNO^{-} + CONH_2^{-} \quad (14)$$

$$CONH^{\cdot -} + O_2 \rightarrow O_2^{\cdot -} + HNCO \quad (15)$$

$$HNCO + OH^{-} \rightarrow H_2O + CNO^{-} \quad (16)$$

In the final step, based on the existing hydroxide radicals in the reaction environment, the cyanate ion produces bicarbonate, nitrate, nitride, and nitrogen gas (reactions 17–19) [2,4]. It was observed that the toxic cyanide compound is converted to a completely safe material at the end of the oxidation process:

$$CNO^{-} + 3OH^{\cdot} \rightarrow HCO_3^{-} + \frac{1}{2}N_2 + H_2O \quad (17)$$

$$CNO^{-} + 6OH^{\cdot} \rightarrow HCO_3^{-} + NO_2^{-} + H^{+} + 2H_2O \quad (18)$$

$$CNO^{-} + 8OH^{\cdot} \rightarrow HCO_3^{-} + NO_3^{-} + H^{+} + 3H_2O \quad (19)$$

## 5. Conclusion

The results of this work revealed that cyanide removal by synthesized $TiO_2$ nanoparticles with anatase/rutile ratio ($A/R$) of 4 has the maximum photocatalytic properties. There also exist different operational parameters affecting the efficacy of these nanoparticles for cyanide removal. According to these results, removal rate of cyanide decreases when concentration is increased, as for concentrations 15 and 100 ppm cyanide was completely degraded during 10 and 90 min. Moreover, for cyanide degradation, the optimum $TiO_2$ content and pH were determined as 1 g $L^{-1}$ and 11, respectively. Furthermore, it was found that the efficiency of removal process corresponds with the increased UV lamp irradiation and $H_2O_2$ dosage. Finally, the photocatalytic degradation trend of cyanide showed that cyanide ion is converted to cyanate and cyanogen in the early stages. However, as photocatalytic process continues, it is converted to components with less toxicity such as bicarbonate, nitrate, nitrite, and nitrogen gas.

## Acknowledgments

The authors would like to thank the management and authorities of Tarbiat Modares University (TMU, Iran Nanotechnology Initiative Council (INIC) and Qaemshahr Branch of Young Researchers Club for their constant support and encouragement.

## References

[1] B. Dąbrowski, A. Zaleska, M. Janczarek, J. Hupka, J.D. Miller, Photo-oxidation of dissolved cyanide using $TiO_2$ catalyst, J. Photochem. Photobiol. A: Chem. 151 (2002) 201–205.
[2] K. Osathaphan, P. Tiyanont, R.A. Yngard, V.K. Sharma, Removal of cyanide in Ni(II)–Cyanide, Ni(II)–cyanide–EDTA, and electroplating rinse wastewater by Ferrate(VI), Water Air Soil Pollut. 219 (2011) 527–534.
[3] A. Bozzi, I. Guasaquillo, J. Kiwi, Accelerated removal of cyanides from industrial effluents by supported $TiO_2$ photo-catalysts, Appl. Catal. B: Environ. 51 (2004) 203–211.
[4] S. Malhotra, M. Pandit, J. Kapoor, D. Tyagi, Photo-oxidation of cyanide in aqueous solution by the UV/$H_2O_2$ process, J. Chem. Technol. Biotechnol. 80 (2005) 13–19.
[5] R.R. Dash, A. Gaur, C. Balomajumder, Cyanide in industrial wastewaters and its removal: A review on biotreatment, J. Hazard. Mater. 163 (2009) 1–11.
[6] R. Ameta, S. Benjamin, A. Ameta, S.C. Ameta, Photocatalytic degradation of organic pollutants: A review, Mater. Sci. Forum Trans. Technol. Publ. 734 (2013) 247–272.

[7] M.M. Botz, Overview of Cyanide Treatment Methods, Mining Environmental Management, Mining Journal Ltd., London, UK, 2001, pp. 28–30.
[8] C. Junin, P. Limthongkul, C. Thanachayanont, Photoactivity of $TiO_2$ films on glass substrate for cyanide degradation, Adv. Mater. Res. 93–94 (2010) 87–90.
[9] C. Karunakaran, P. Gomathisankar, G. Manikandan, Solar photocatalytic detoxification of cyanide by different forms of $TiO_2$, Korean J. Chem. Eng. 28 (2011) 1214–1220.
[10] E. Ozcan, Z. Gok, E. Yel, Photo/photochemical oxidation of cyanide and metal–cyanide complexes: Ultraviolet A versus ultraviolet C, Environm. Technol. 33 (2012) 1913–1925.
[11] Y.L Li, T. Ishigaki, Controlled one-step synthesis of nanocrystalline anatase and rutile $TiO_2$ powders by in-flight thermal plasma oxidation, J. Phys. Chem. B 108 (2004) 15536–15542.
[12] A. Khataee, V. Vatanpour, A. Amani Ghadim, Decolorization of CI Acid Blue 9 solution by UV/Nano-$TiO_2$, Fenton, Fenton-like, electro-Fenton and electrocoagulation processes: A comparative study, J. Hazard. Mater. 161 (2009) 1225–1233.
[13] M.S. Siboni, M.T. Samadi, J.K. Yang, S.M. Lee, Photocatalytic reduction of Cr(VI) and Ni(II) in aqueous solution by synthesized nanoparticle ZnO under ultraviolet light irradiation: A kinetic study, Environ. Technol. 32 (2011) 1573–1579.
[14] J.K. Yang, S.M. Lee, M. Farrokhi, O. Giahi, M. Shirzad, Photocatalytic removal of Cr(VI) with illuminated $TiO_2$, Desalin. Water Treat. 46 (2012) 375–380.
[15] V. Augugliaro, V. Loddo, G. Marcì, L. Palmisano, M.J. López-Muñoz, Photocatalytic oxidation of cyanides in aqueous titanium dioxide suspensions, J. Catal. 166 (1997) 272–283.
[16] M. Barakat, Y. Chen, C. Huang, Removal of toxic cyanide and Cu(II) Ions from water by illuminated $TiO_2$ catalyst, Appl. Catal. B: Environ. 53 (2004) 13–20.
[17] K. Chiang, R. Amal, T. Tran, Photocatalytic degradation of cyanide using titanium dioxide modified with copper oxide, Adv. Environ. Res. 6 (2002) 471–485.
[18] N. Costarramone, A. Kneip, A. Castetbon, Ferrate(VI) oxidation of cyanide in water, Environ. Technol. 25 (2004) 945–955.
[19] I. Ibrahim, A. Ismail, R. Mohamed, Degradation of free cyanide by photocatalytic oxidation, Eur. J. Miner. Process. Environ. Prot. 3 (2003) 281–290.
[20] B.K. Mert, Ö. Sivrioğlu, T. Yonar, S′. Özçiftçi, Treatment of jewelry manufacturing effluent containing cyanide using ozone-based photochemical advanced oxidation processes, Ozone: Sci. Eng. 36 (2014) 196–205.
[21] M. Motegh, J.R. van Ommen, P.W. Appel, M.T. Kreutzer, Scale-up study of a multiphase photocatalytic reactor degradation of cyanide in water over $TiO_2$, Environ. Sci. Technol. 48 (2014) 1574–1581.
[22] R.A. Wahaab, A.K. Moawad, E.A. Taleb, H.S. Ibrahim, H.A.H. El-Nazer, Combined photocatalytic oxidation and chemical coagulation for cyanide and heavy metals removal from electroplating wastewater, World Appl. Sci. J. 8 (2010) 462–469.
[23] M. Farrokhi, J.K. Yang, S.M. Lee, M. Shirzad-Siboni, Effect of organic matter on cyanide removal by illuminated titanium dioxide or zinc oxide nanoparticles, J. Environ. Health Sci. Eng. 14 (2013) 11–23.
[24] M.S. Siboni, M.R. Samarghandi, J.K. Yang, S.M. Lee, Photocatalytic removal of cyanide with illuminated $TiO_2$, Water Sci. Technol. 64 (2011) 1383–1387.
[25] S.H. Kim, J.W. Seol, W.C. Lee, S.W. Lee, S.O. Kim, Photocatalytic oxidation of free cyanide using UV LED, J. Korean Sci. Environ. Eng. 37 (2015) 34–44.
[26] M. Motegh, J.R. Ommen, P.W. Appel, M.T. Kreutzer, Scale-up study of a multiphase photocatalytic reactor —degradation of cyanide in water over $TiO_2$, Environ. Sci. Technol. 48 (2014) 1574–1581.
[27] B.K. Mert, O. Sivrioğlu, T. Yonar, S. Özçiftçi, Treatment of jewelry manufacturing effluent containing cyanide using ozone-based photochemical advanced oxidation processes, J. Int. Ozone Assoc. 36 (2014) 11–23.
[28] H. Ijadpanah Saravy, M. Safary, A. Khodadadi, M. Rezaee, Synthesis of titanium dioxide nanoparticles for photocatalytic degradation of cyanide in wastewater, Anal. Lett. 47 (2013) 1772–1782.
[29] S. Kittaka, K. Matsuno, S. Takahara, Transformation of ultrafine titanium dioxide particles from rutile to anatase at negatively charged colloid surfaces, J. Solid State Chem. 132 (1997) 447–450.
[30] A. Sun, P. Guo, Z. Li, Y. Li, P. Cui, Low temperature synthesis of anatase and rutile titania nanopowders by hydrolysis of $TiCl_4$ using ammonia gas, J. Alloys Compds. 481 (2009) 605–609.
[31] A. Patterson, The Scherrer formula for X-ray particle size determination, Phys. Rev. 56 (1939) 978.
[32] Methods for the Examination of Water and Wastewater, 20th ed., American Public Health Association/American Water Works Association/Water and Environmen Federation, Washington, DC , (1998).
[33] J.H. Lee, Y.S. Yang, Effect of HCl concentration and reaction time on the change in the crystalline state of $TiO_2$ prepared from aqueous $TiCl_4$ solution by precipitation, J. Eur. Ceram. Soc. 25 (2005) 3573–3578.